

## SYNTHESIS AND ANTIMICROBIAL ACTIVITY OF NANOCOMPOSITES OF POLYANILINE AND SILVER NANOPARTICLES VIA SELF-ASSEMBLY METHOD

D. Rama Devi<sup>1</sup>, B. Ganga Rao<sup>1</sup> and K. Basavaiah<sup>2</sup>

<sup>1</sup>A.U. College of Pharmaceutical Sciences, Andhra University, Visakhapatnam, India.

<sup>2</sup>Department of Inorganic and Analytical Chemistry, Andhra University, Visakhapatnam, India.

Article Received on  
09 Sept. 2016,

Revised on 29 Sept. 2016,  
Accepted on 20 October 2016

DOI: 10.20959/wjpps201611-7791

### \*Corresponding Author

**D. Rama Devi**

A.U. College of  
Pharmaceutical Sciences,  
Andhra University,  
Visakhapatnam, India.

### ABSTRACT

Nanocomposites of conducting polymer Polyaniline (PANI) and silver nanoparticles (Ag NPs) have been prepared via chemical oxidative polymerization of monomer using AgNO<sub>3</sub> as an oxidant in presence of CSA without using any external oxidizing and reducing agents. As prepared nanocomposites of CSA doped PANI/Ag NP have been characterized by range of spectroscopy as well as microscopy techniques such as UV-vis spectroscopy, FTIR spectroscopy, X-Ray diffraction (XRD), scanning electron microscopy (SEM), and transmission electron microscopy (TEM). The thermal stability of nanocomposite of PANI/Ag NPs was investigated by

thermogravimetry analysis (TGA). The XRD patterns indicated that the crystalline phase of Ag NPs is cubic. The TEM image shows that the Ag NPs are well dispersed in the PANI nanostructures. The CSA doped PANI/Ag NPs nanocomposites show excellent an antimicrobial activity against *staphylococcus aureus*.

**KEYWORDS:** Silver nanoparticles, Polyaniline, Nanocomposites, oxidative chemical polymerization, Antimicrobial activity.

### 1. INTRODUCTION

In recent years, metal nanoparticles have attracted great attention owing to their optical and electronic properties related with the quantum size effect and many technologic applications in optics, optoelectronics, catalysis, nanostructure fabrication and sensor.<sup>[1]</sup> Among these, silver nanoparticles (Ag NPs) have emerged as potential candidates for technological

applications such as catalysis, conductive inks, thick film pastes and adhesives for various electronic components, anti-fungal, anti-inflammatory, anti-viral, and an effective antimicrobial agent against various pathogenic microorganisms due to their unique electrical and optical properties.<sup>[2–8]</sup>

Most of these applications require well dispersed and agglomerate free Ag NPs with particle size less than critical particle size. However, Ag NPs can easily agglomerate due to dipole/dipole interaction and Vander Waal's attractive forces between the nanoparticles. Hence, aggregation of Ag NPs limits in many instances their practical application in various fields. Numerous methods have been developed for stabilization of Ag NPs by using various coating materials. One of the main approaches to overcome these limitations is to protect the Ag NPs by capping using capping agents such as polymers, silica and inorganic metals oxides. The capping agent not only prevents the aggregation Ag NPs but also provides a useful platform for further functionalization. Especially, the polymeric capping agent not only to prevent Ag NPs aggregation but also controls the particle sizes and shape. Ag NPs protected by polymers such as poly (vinyl alcohol) (PVA), poly (vinylpyrrolidone) (PVP), polystyrene (PS) or poly (methyl methacrylate) (PMMA) and conducting polymers have been extensively reported. Among conducting polymers, polyaniline (PANI) has received more attention for its easy synthesis, low monomer cost, good environmental stability, and relatively high conductivity, unique redox property useful for potential technological applications in electromagnetic interference shielding, electrochromic devices, sensing and actuating technologies, nonlinear optical systems, and molecular engineering of nanodevices. Moreover, nanocomposites of PANI / metal nanoparticles composite as they combine the properties of the low dimensional organic conductors and high surface area, and numerous applications of PANI, as well as the unique optical and catalytic properties of metal nanoparticles. However, the solution processing of PANI is difficult due to the presence of intra chain and inters chain H-bonding interactions of N-quinonoid and benzenoid moieties of PANI. It is therefore desirable to develop a method for solution processibility of PANI with simultaneous capping of metal nanoparticles in nanocomposites

In recent years, many new drugs have been introduced to tackle the growing menace of the continuing appearance of antibiotic resistance in pathogenic and opportunistic microorganisms. However, none of them have improved activity against multidrug-resistant bacteria. Since, Ag NPs and their nanocomposites have been used to reduce the microbial

infection in burn wound and prevention of bacterial colonization on various surfaces such as catheters, prostheses. Therefore, in present study the synthesized nanocomposite of CSA doped PANI/Ag NPs was used to test their antibacterial activity against gram positive model organism.

In the present study, CSA doped PANI / Ag NPs nanocomposites have been synthesized via *in-situ* self-assembly method using  $\text{AgNO}_3$  as an oxidant in presence of CSA without using any external oxidizing and reducing agents. As synthesized PANI/Ag nanocomposites have been characterized by using UV-Vis, XRD, FTIR, SEM- EDX and TEM. The effect of Ag NPs on thermal stability of nanocomposites has been studied by thermogravimetric analysis (TGA). We report the synthesis and characterization of a novel class of that acts as an efficient anti-microbial agent. The main focus in this study is synthesis, characterization, and antimicrobial activity of CSA doped PANI/ Ag NPs. Antimicrobial activity were investigated against on bacterial strains of *E. coli* and *S. aureus* to evaluate the efficacy of the generated CSA doped PANI/ Ag NPs for their potential biomedical applications. Further, we note that the synthetic procedure followed in this work can provide a very general route to the synthesis of diversely useful composites of PANI with other metal nanoparticles.

## 2. MATERIALS AND METHODS

### 2.1. Materials

Silver nitrate ( $\text{AgNO}_3$ , 99.9% Aldrich grade), aniline monomer (99% purity) double distilled under reduced pressure and stored at low temperature prior to use. Oxidizing agent Ammonium persulphate(APS) and camphor sulphonic acid(CSA) were purchased from Aldrich and used as received. Dimethylsulfonamide (DMSO), Agar were used as received. All the solutions were prepared using double distilled water during the synthesis.

### 2.2. Synthesis of CSA doped PANI/ Ag NPs

In typical synthesis process, 0.0736 g of aniline (0.04 M) was dissolved in 10 ml of distilled water taken in a round bottom flask under ultra-sonication for 1h. To this, a 10 ml of CSA (0.02M) solution was added under vigorous stirring. The reaction mixture was quickly cooled to 0-5 °C with constant stirring for 2 h to obtain a milky dispersion of particles of anilinium-CSA complex. A pre-cooled solution of 10 ml aqueous  $\text{AgNO}_3$  (0.02 M) was then added drop wise to the above solution under vigorous stirring 0-5 °C. The reaction mixture was then stirred for an additional 5h at 0-5°C when the colour of reaction mixture slowly turns through light blue to dark green, indicating the formation of CSA doped PANI. The reaction was

further allowed to proceed for 24 h under stirring. AgNO<sub>3</sub> present in the reaction mixture was reduced into Ag NPs by as formed PANI and then mixture was centrifuged, washed with distilled water and finally with methanol. The product was then dried under vacuum at room temperature for 12 h. Same procedure has been adopted for the preparation of other CSA doped PANI / Ag NPs nanocomposites, with different molar ratio of aniline to CSA of 1:1, 1:2, 1:3, 1:4, and 1:5.

### 2.3. Characterization

The morphology was examined by scanning electron microscopy (SEM) on JEOL-JSM6610 LV equipped with an electron probe- micro analyzer. Energy dispersive X-ray (EDAX) measurement was also performed on the same equipment to determine chemical composition. Transmission electron microscopy image was obtained [TEM model FEI TECNAI G2 S-Twin] at accelerating voltages of 120 and 200 kV. X-ray diffraction (XRD) pattern were measurement was performed by using using a Siemens AXS D5005 X-ray diffract meter at 1degree per minute with Cu-K $\alpha$  radiation. Fourier transform infrared (FTIR) spectra were recorded over the range of 400-4000 cm<sup>-1</sup> using a Perkin Elmer SPECTRUM 1000 FTIR Spectrometer. The powder samples were mixed thoroughly with KBr and pressed into thin pellets. For UV-Visible absorption spectra the samples were dissolved in dimethylsulphoxide (DMSO) and spectra were recorded on a Perkin-Elmer double beam LS-50 spectrophotometer. Thermogravimetric analysis (TGA) was carried out using in a TGA, Cahn TG131 system with heating rate of 20 °C min<sup>-1</sup> under N<sub>2</sub> atmosphere.

### 2.4. Antimicrobial activity studies

#### Screening for Antibacterial Activity

The antibacterial activity was performed by using model organisms, a gram positive *Staphylococcus aureus* in Nutrient Agar medium. The medium was sterilized by autoclaving at 120<sup>0</sup>C (15 lb/in<sup>2</sup>). About 30 ml of the medium (Nutrient Agar Medium) with the strains of bacteria was transferred aseptically into each sterilized Petri plate. The Plates were left at room temperature for solidification. Each plate, a single well of 6 mm diameter was made using a sterile borer. The CSA doped PANI /Ag nanocomposites were freshly reconstituted with dimethyl sulphoxide and tested at various concentrations. The samples and the control (0.1 ml) were places in 6-mm diameter well. Antibacterial assay plates were incubated at 37 $\pm$  2)<sup>0</sup>C for 24 h. Standard with Ciproflaxin (5 $\mu$ g/ml) was used as a positive control for

antibacterial activity. Each experiment was carried out in triplicates, and diameter of the zone of inhibition was measured.

### 2.5. Determination of minimum inhibitory concentration

Antimicrobial activity of the as synthesized CSA doped PANI/Ag nanocomposites was investigated using agar-well diffusion method. The medium was sterilized by autoclaving at 120 °C (15 lb/in<sup>2</sup>). About 30 ml of the medium (Nutrient agar medium) with the strains of bacteria was transferred aseptically into each sterilized petri plate. The plates were left at room temperature for solidification. Each plate, a single well of 6 mm diameter was made using a sterile borer. The extracts were freshly reconstituted with Dimethyl Sulphoxide and tested at various concentrations. The samples and the control (0.1 ml) were placed in 6-mm diameter well. Antibacterial assay plates were incubated at 37± 2°C for 24 h. Standard with Ciproflaxin (5µg/ml) was used as a positive control for antibacterial activity. Each experiment was carried out in triplicates, and diameter of the zone of inhibition was measured.

## 3. RESULTS AND DISCUSSIONS

The synthesis of CSA doped PANI / Ag NPs nanocomposite is based on *in-situ* oxidative chemical polymerization of monomer in an acidic environment using AgNO<sub>3</sub> as an oxidant in the presence of excess of CSA as dopant. Firstly, AgNO<sub>3</sub> being oxidizing agent induces the polymerization of monomer to PANI, which in turn reduces AgNO<sub>3</sub> to Ag NPs and thus encapsulated by the PANI matrix. In this synthesis, CSA act as dopant and surfactant due to its hydrophilic group (-SO<sub>3</sub>H) and hydrophobic group and hence CSA easily forms micelles in an aqueous solution. Besides, CSA being acidic form dopant-aniline salts, which act as “soft template” for growth of PANI nanostructures. The presence of excess CSA can prevent the formation of larger particles via steric hindrance and thereby producing nanometre sized PANI. Ag NPs were also formed inside CSA micelles “reactor” during the sedimentation process and decorated on the PANI. CSA having -SO<sub>3</sub><sup>-</sup> group can stabilize Ag NPs and thus to protect the NPs from aggregations.

UV-visible absorption spectra of CSA doped PANI / Ag nanocomposite were depicted in Fig. 1. The absorption spectrum of PANI/Ag nanocomposite displayed characteristic absorption at 290, 340 and 520 nm. The peak at ≈ 520 nm corresponds to the SPR of the Ag NPs embedded in the PANI matrix which was over-lapped by the polaronic peak of PANI appearing at same wavelength. Absorption peaks at 340 nm have been assigned to  $\pi \rightarrow \pi^*$

transition of benzenoid rings in the PANI chain. Both absorption peaks were shifted from those of pure PANI indicating that there is some interaction between Ag NPs and PANI backbones. Besides these two peaks, there is a sharp peak at 290 nm due to the  $\pi \rightarrow \pi^*$  transition in the benzenoid rings of CSA, which confirms the presence of CSA in the nanocomposites.

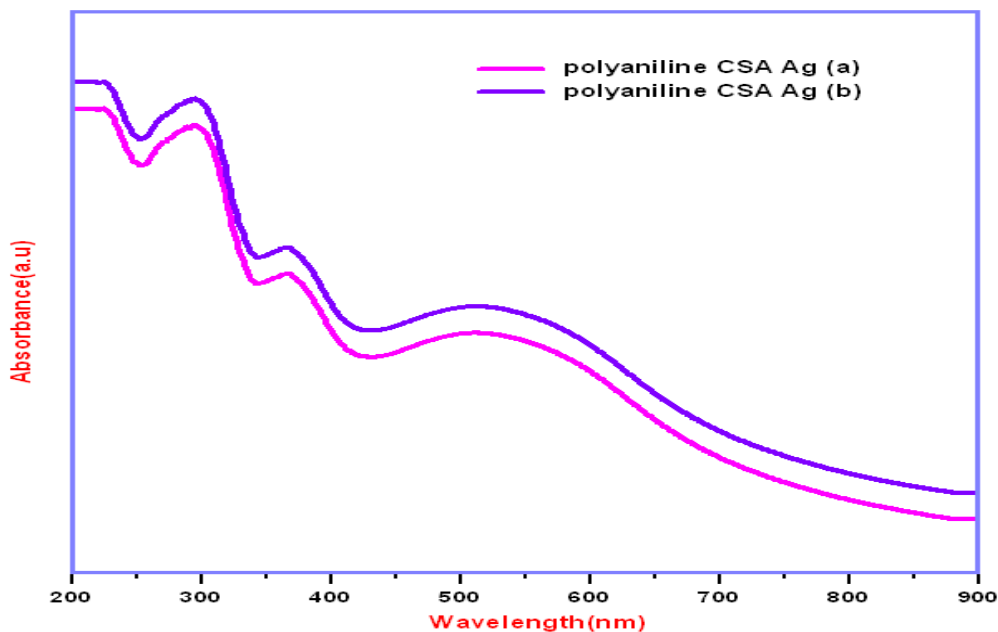


**Fig.2.** UV-Visible spectra of CSA doped PANI/Ag nanocomposites prepared at 1:1 and 1:2 molar ratios of aniline to CSA

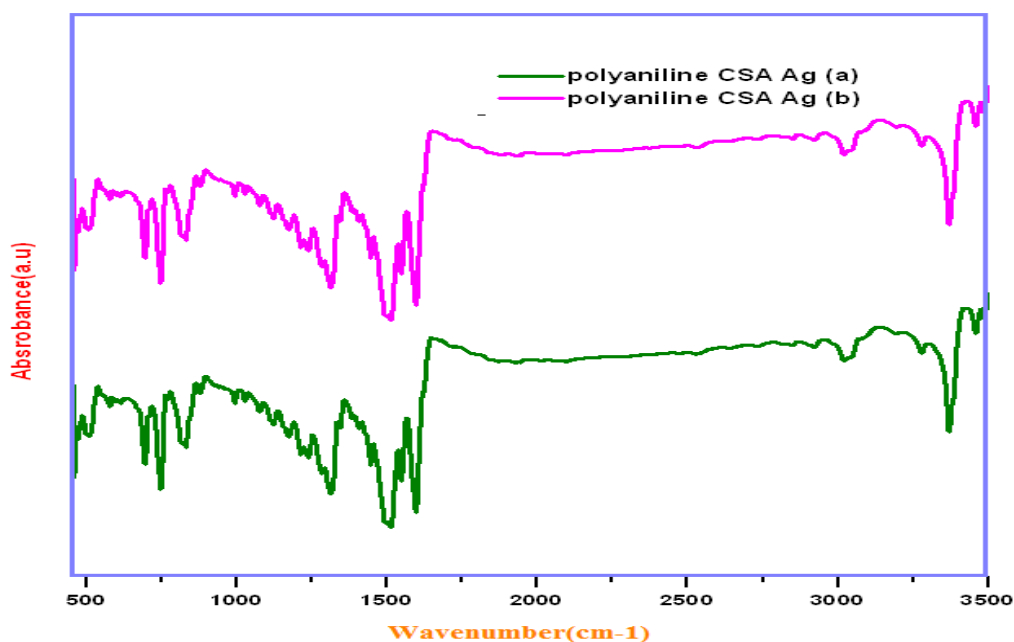


**Fig.3.** FTIR spectra of CSA doped PANI/Ag nanocomposites prepared at 1:1 and 1:2 molar ratios of aniline to CSA

FTIR spectra of PANI/Ag nanocomposite prepared at 1:1 and 1:2 molar ratios of monomer to CSA were presented in Fig.2, which are in complete agreement with previously reported literature. The characteristic peaks at  $1557\text{ cm}^{-1}$  and  $1454\text{ cm}^{-1}$  were assigned to C- N stretching of the quinoid and the C- C stretching of the benzoid rings, respectively. The broad band in the region between  $3100$  and  $3650\text{ cm}^{-1}$  corresponds to stretching of N-H bond. A sharp peak observed at  $3436\text{ cm}^{-1}$  was due to the N-H stretching vibrations. The appearance of a broad band instead of a sharp peak is due to the presence of a high concentration of N-H groups in the nanocomposite. The absorption peaks around  $2850$  and  $2992\text{ cm}^{-1}$  correspond to C-H stretching vibrations, whereas the absorption peak at  $\sim 1384\text{ cm}^{-1}$  can be assigned to aromatic C-N stretching vibrations. The peaks around  $1176$  and  $1041\text{ cm}^{-1}$  correspond to stretching vibrations of the  $\text{SO}_3\text{H}^-$  group.<sup>[37]</sup> The characteristic band centred at  $666\text{ cm}^{-1}$  corresponds to the C-S stretching of the benzenoid ring of CSA.

Fig. 3 shows the powder XRD pattern of PANI / Ag nanocomposite prepared at two synthesized via *in-situ* chemical polymerization method. The broad peak at  $2\theta = 19.85$  can be attributed to the periodicity parallel to the amorphous polymer chain, while the sharp peaks at  $2\theta$  values  $38.17$ ,  $44.36$ ,  $64.51$  and  $77.46$  can be assigned to the face centered cubic (fcc) phase of silver (111), (200), (220) and (311), respectively and are in good agreement with the reported data (JCPDS File No. 06-0480). The existence of sharp peaks clearly indicates the presence of Ag NPs in the composites with their crystalline nature. The broad peak at  $2\theta$  value at  $10\text{--}35$  is due to amorphous nature of PANI.

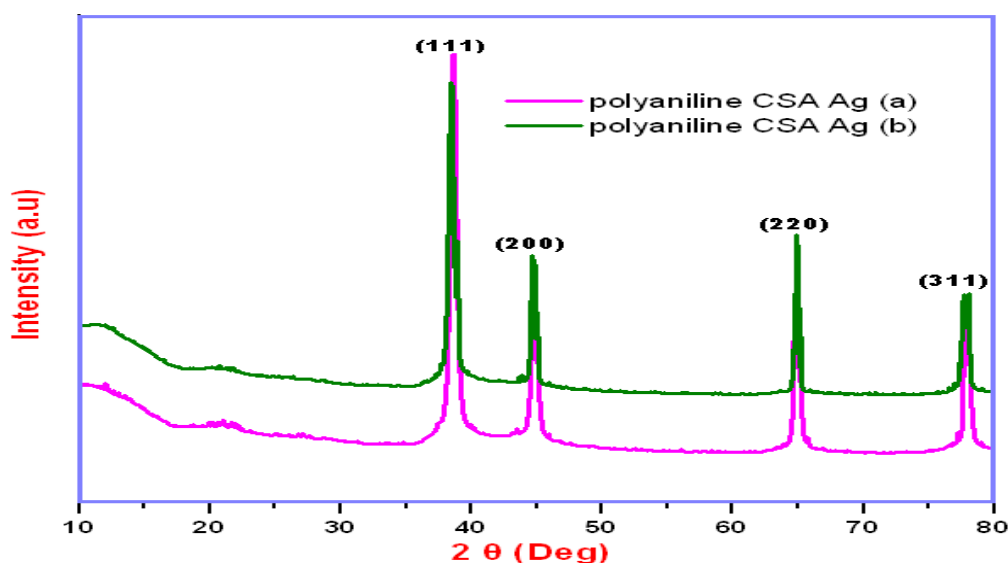
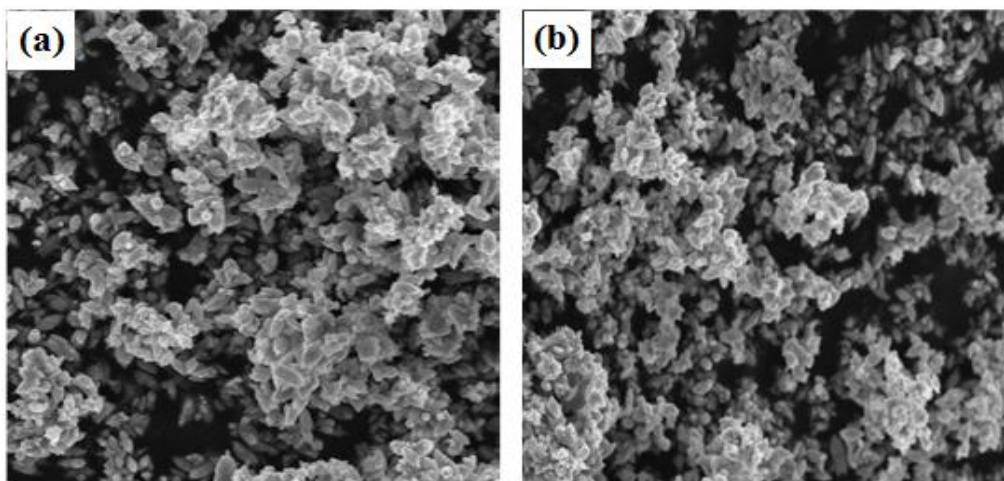


Fig.4. Powder XRD patterns of CSA doped PANI/Ag nanocomposites prepared at 1:1 and 1:2 molar ratios of aniline to CSA.

The morphology of PANI / Ag NPs nanocomposites was investigated SEM and TEM. Fig.4 shows the SEM image of PANI/Ag nanocomposite prepared using  $\text{AgNO}_3$  as oxidant in presence of CSA. Fig.4 clearly shows the tube like morphology and large number of Ag NPs coated on PANI. It is found that the morphology composites critically dependent upon molar ratio of aniline to CSA.



**Fig: 5. Scanning electron microscopy images of CSA doped PANI/Ag NPs nanocomposites prepared at (a) 1:1 and (b) 1:2 molar ratios of aniline to CSA**

Transmission electron microscopy (TEM) image of as prepared PANI/Ag NPs nanocomposites displayed in Fig.5, shows Ag NPs are nearly spherical with an average diameter ranges from 3-7 nm. It can be seen that the vast majority of particles exhibit a diameter close to 3-7 nm without particles aggregation, because as synthesized Ag nanoparticles were coated with CSA.

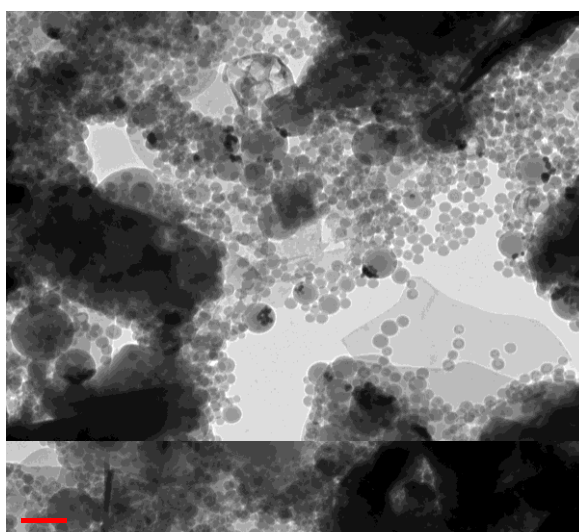


**Fig: 7 Transmission electron image of CSA doped PANI/ Ag NPs nanocomposites.**



Thermal stability of CSA doped PANI / Ag nanocomposite was investigated by TGA analysis and the corresponding thermogram was presented in Fig. 8. The thermogram was recorded from room temperature-850°C in an inert (N<sub>2</sub>) atmosphere with heating rate of 20°C/min. It was observed that PANI/ Ag nanocomposite undergoes three step decomposition patterns similar to pure PANI. In the first step of degradation (100°C), a small fraction of weight loss occurred, which is due to the removal of water molecules or moisture that might be present in nanocomposite. The second step of weight loss occurs in the temperature range of 220–345°C is due to the removal (thermal dedoping) of acid dopant, CSA. In the third step of decomposition process, a rapid weight loss in the temperature range of 350–550°C was observed, which is due to thermal oxidative decomposition and degradation of the polymer fraction of nanocomposite. It was seen that the nanocomposites have a greater thermal stability than the pure polymers. This higher thermal stability of the nanocomposite was probably due to the presence of Ag NPs, which control thermal motion of the polymer matrix in the composite.

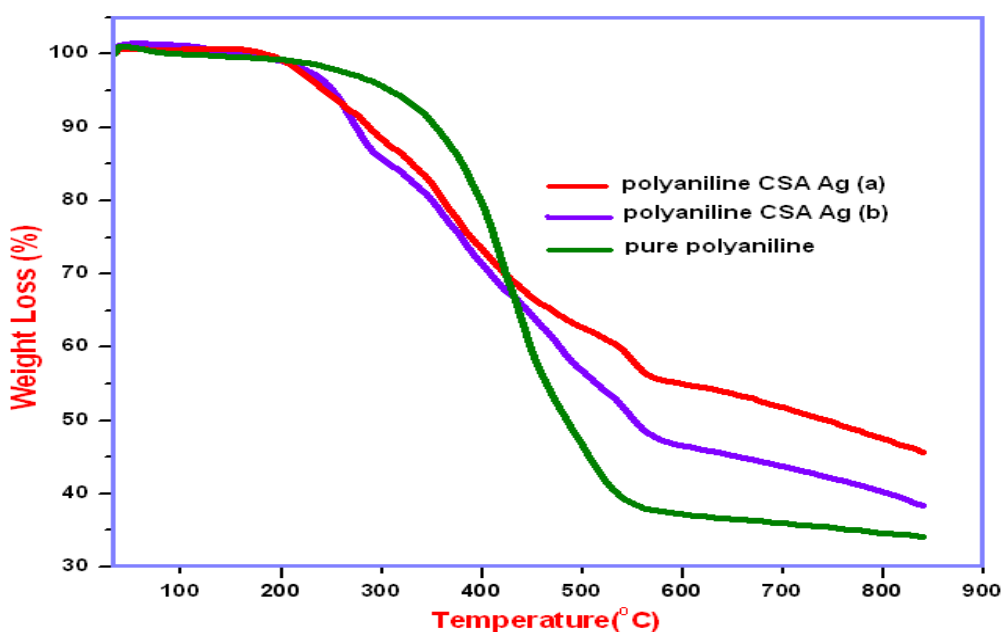


**Fig. 8** Thermogravimetry analysis of (a) pure PANI and (b, c) PANI/Ag NPs nanocomposites prepared at 1:1 and 1:2 molar ratios of aniline to CSA.

#### Antimicrobial studies

In an effort to tackle the growing menace of the continuing appearance of antibiotic resistance in pathogenic and opportunistic microorganisms, many new drugs were introduced in recent years, however, none of them have improved activity against multidrug-resistant

bacteria. Since, silver nanoparticles and their composites have been used to reduce the microbial infection in burn wound and prevention of bacterial colonization on various surfaces devices such as catheters, prostheses, hence in present study, the synthesized PANI /Ag nanocomposite was used to test their antibacterial activity against gram positive model organism, *Staphylococcus aureus*. Each experiment was carried out in triplicates, and diameter of the zone of inhibition was measured. Observations and results are shown in Table 1.

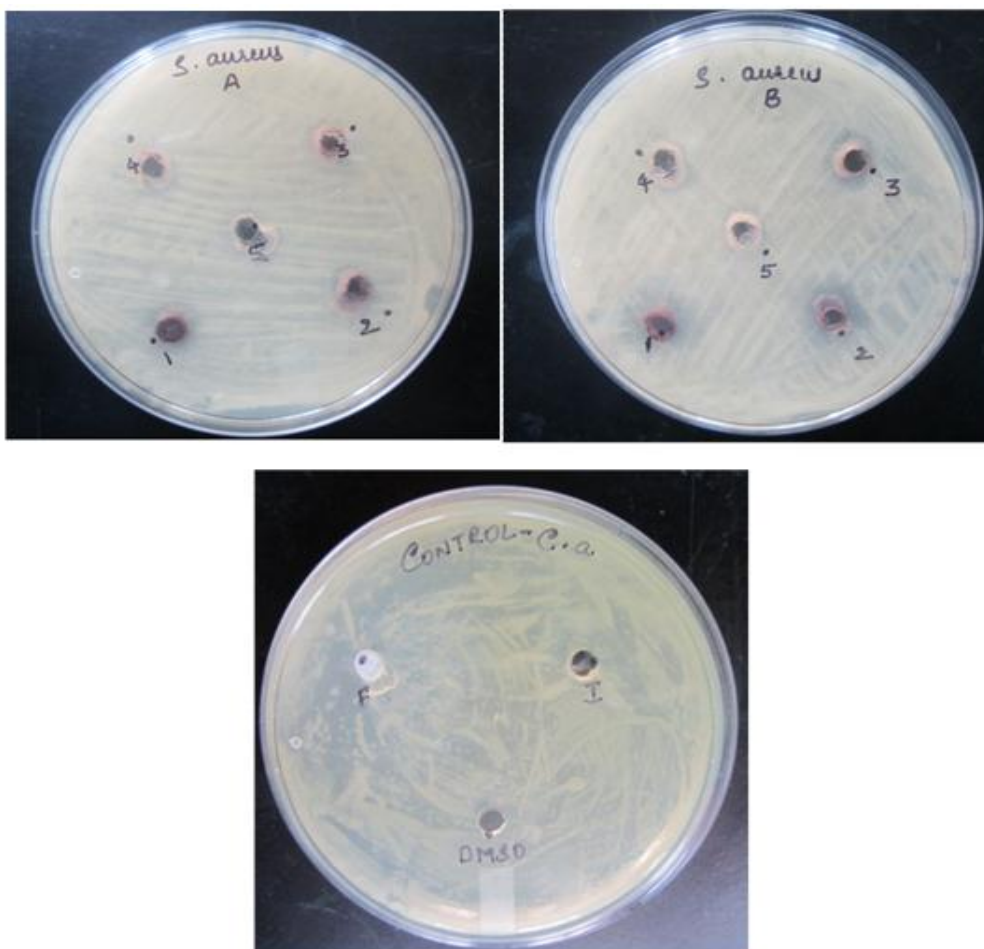


**Fig: 9 Images of antimicrobial activity inhibition zone of nanocomposites of CSA doped PANI and Ag NPs against *S. Aureus*.**

**Table: 1 The zone of inhibition of CSA doped PANI and Ag nanocomposites against *S. Aureus*.**

Organism	CSA doped PANI-Ag (A)	CSA doped PANI-Ag (B)	Control (Ciproflaxin)
<i>S. aureus</i>	12 mm	09 mm	24 mm

The extracts that showed antimicrobial activity were subjected to minimum inhibitory concentration (MIC) assay by serial two fold dilution method. MIC was interpreted as the

lowest concentration of the sample, which showed clear fluid without development of turbidity.

## CONCLUSIONS

In conclusion, CSA doped PANI / Ag NPs nanocomposites have been synthesized via *in-situ* self-assembly method using AgNO<sub>3</sub> as an oxidant in presence of CSA. The spectroscopic data revealed that the successful formation of PANI/Ag nanocomposites. SEM and TEM images clearly show the Ag NP adsorbed on surface of PANI nanostructures. It is found that the morphology of nanocomposites is dependent on the molar ratios of monomer to CSA. TGA data indicated that Ag NPs enhanced the thermal stability of composites. The antibacterial activity of nanocomposite was performed by using model organisms, *Staphylococcus aureus* in Agar medium. Excellent antibacterial activity was observed for CSA doped PANI /Ag nanocomposite.

## REFERENCES

1. Wiley BJ, Im SH, Li ZY, McLellan J, Siekkinen A, Xia Y. Maneuvering the surface plasmon resonance of silver nanostructures through shape-controlled synthesis. *J. Phys. Chem. B*, 2006; 110(32): 15666–75.
2. Ramirez IM, Bashir S, Luo Z, Liu JL. Green synthesis and characterization of polymer-stabilized silver nanoparticles. *Colloids Surf. B: Biointerfaces*, 2009; 73(2): 185–91.
3. Panacek A, Kolar M, Vecerova R, Pucek R, Soukupova J, Krystof V, Hamal P, Zboril R, Kvitek L. Antifungal activity of silver nanoparticles against *Candida* spp. *Biomaterials*, 2009; 30(31): 6333–40.
4. Nadworny PL, Wang J, Tredget EE, Burrell RE. Anti-inflammatory activity of nanocrystalline silver in a porcine contact dermatitis model. *Nanomed. Nanotechnol. Biol. Med.*, 2008; 4(3): 241–51.
5. Rogers JV, Parkinson CV, Choi TW, Speshock JL, Hussain SM. A Preliminary Assessment of Silver Nanoparticle Inhibition of Monkeypox Virus Plaque Formation. *Nanoscale Res. Lett.*, 2008; 3(4): 129–33.
6. Gurunathan S, Lee KJ, Kalishwaralal K, Sheikpranbabu S, Vaidyanathan R, Eom SH. Antiangiogenic properties of silver nanoparticles. *Biomaterials*, 2009; 30(31): 6341–50.
7. Duran N, De Souza GIH, Alves OL, Esposito E, Marcato PD. Antibacterial activity of silver nanoparticles Synthesized by *Fusarium oxysporum* strain. *J. Nanotechnol*, 2003; 122–128.